



Finite Element Simulation of Metal Cutting of Aluminum using Johnson-Cook Damage Model and Shear Failure Model

محاكاة عملية قطع الألومنيوم باستخدام طريقة العناصر المحدودة ونموذجي جونسون كوك والقص لانهايار المعادن

Mohammed Saber

KEYWORDS:

Finite element method, metal cutting, simulation, chip formation, ductile damage model, shear failure model, Al 1100

الملخص العربي: يتناول هذا البحث استخدام نموذج جونسون-كوك لانهايار المعادن وكذا استخدام نموذج القص في طريقة العناصر المحدودة اثناء محاكاة لعمليات قطع سبيكة الومنيوم (Al 1100) باستخدام برنامج أباكوس. بالنسبة لنموذج جونسون-كوك، فإن متغير "الإزاحة عند الانهيار"، بالإضافة إلى حجم العناصر في منطقة الرانش، لهم تأثير كبير على شكل الرانش الناتج من عملية محاكاة القطع وكذا له تأثير على شكل الرانش ومدى اكتمال التحليل. ولذلك توصي الدراسة بتثبيت حجم العناصر في منطقة الرانش إلى متوسط حجم الحبيبات لمادة الشغلة مع تكرار استخدام قيم مختلفة من المتغير "الإزاحة عند الانهيار" ومقارنة الرانش الناتج برانش تم الحصول عليه من التجارب المعملية حتى يتم التوافق بين رانش المحاكاة ورنش التجارب وحينئذ تكون قيمة "الإزاحة عند الانهيار" هي القيمة الصحيحة. كما يتضمن البحث أيضاً استخدام نموذج القص لمحاكاة عملية قطع الألومنيوم ومقارنة النتائج المتحصل عليها من هذا النموذج مع النتائج المتحصل عليها من استخدام نموذج جونسون كوك ووجد توافق جيد بينهما. وبالتالي فإنه يقترح استخدام نموذج القص في عملية محاكاة القطع لسهولة حيث انه لا يحتاج الى تحديد قيمة "الإزاحة عند الانهيار"، كما يتطلب ذلك نموذج جونسون كوك.

Abstract— This paper evaluates the use of the Johnson-Cook (J-C) damage model and the shear failure model in the Finite Element metal cutting simulations of an Aluminum alloy (Al 1100) using an FE commercial package ABAQUS. For the J-C model, the damage evolution in the model is controlled by the value of the parameter "equivalent plastic displacement at failure", \bar{u}_f^{pl} . The value of this parameter is provided to ABAQUS by user. It was found that the value of that parameter, in conjunction with mesh size, highly affects the chip morphology, chip ratio and analysis completion. Therefore, a compromising between the value of \bar{u}_f^{pl} and the mesh size used should be done. The proper value of the \bar{u}_f^{pl} depends on the

mesh size in the chip zone of the model. Therefore, it is suggested to select the element size, of chip zone of the model, almost equals to the average grain size of workpiece. Then, change the values of \bar{u}_f^{pl} until the obtained FE results agree well with experimentally formed chip. As an alternative to the use of J-C damage model, shear failure model was also used. The use of the shear failure model does not need a definition of a damage parameter to conduct the cutting simulations. The results obtained from the J-C damage model, with tuned \bar{u}_f^{pl} , are in good agreement with those obtained using the shear failure model. However, those results are meshing dependent in both models. Therefore, qualitative comparison of the simulated chip with experimental chip is still necessary.

Received: 7 November, 2016 - revised: 27 December, 2016 - accepted: 29 May, 2017.

Mohammed Saber, Assistant Professor at the Department of Production Engineering and Mechanical Design, Faculty of Engineering, Port Said University, Port Fouad, Port Said, Egypt. (e-mail: mssaber77@yahoo.com.).

I. INTRODUCTION

Cutting process is a metal forming process during which the material experiences high strain and high strain rates. It can be modelled using the FE method in conjunction with damage models. In the used FE package,

ABAQUS, the material damage models are the progressive damage models and the dynamic failure damage models. In progressive damage models, several damage initiation criteria, such as ductile, shear, forming limit diagram (FLD), forming limit stress diagram (FLSD), Müschenborn-Sonne forming limit diagram (MSFLD), and Marciniak-Kuczynski (M-K), Johnson-Cook (J-C) and Marciniak-Kuczynski (M-K), are applied[1]. These criteria are used to calculate the damage initiation parameter, e.g. equivalent plastic strain at failure, ϵ_f^{pl} . Once, the equivalent plastic strain, ϵ_{pl} , at an integration point of an element reaches the value of ϵ_f^{pl} , the damage in that element started. However, a damage evolution law is needed to allow the gradual degradation of the material stiffness. If no damage law is used, no stiffness degradation will take place. The values of the parameters of the damage evolution greatly affect the results of the simulation.

On the other hand, dynamic failure damage models do not need a damage evolution law to degrade the material stiffness; once the damage is initiated the element is failed. Again, a damage initiation criterion, such as J-C damage model must be used. The dynamic failure model was designed mainly for high-strain-rate dynamic problems.

In order to model the material flow in metal cutting process, a plasticity model is needed. Johnson-Cook (J-C) plasticity model [2] was used to model the plastic (flow) behavior of a material under high strains and high strain rates, e.g. [3-6].

One of the most controversial issues in metal cutting simulations is the modeling of chip formation (separation). Different approaches were used. Either Eulerian formulation, Lagrangian formulation, Arbitrary Lagrangian Eulerian (ALE) formulation or Combined Eulerian Lagrangian formulation can be used. Many models use a predetermined cutting line along which nodal separation or element failure takes place. [e.g. [7]]. Nodal separation is achieved through the generation of new nodes or the release of boundary conditions on the cutting plane once the separation criterion is met. Others apply a layer of very thin elements, such that it does not affect the analysis on its removal, between the chip and the work piece. Once the damage parameter in those elements reaches 1.0 the element failed and is removed from the analysis. This enables the separation of the chip from the work piece e.g. [7, 8]. This layer of very thin elements is known as sacrificial elements.

Özel and Zeren [5] modelled the chip formation as the flow of the material around the cutting edge. The ALE adaptive meshing enabled them to model chip flow around the tool tip avoiding excessive deformation of the elements, see Figure 1. The advantage of this approach, to Özel and Zeren [5], is the needless of a fracture criterion of the chip separation. Öpöz and Chen [6], used the ALE adaptive meshing in conjunction with J-C plasticity model combined with J-C damage model in simulating grinding process. Although the use of ALE adaptive meshing enabled them to conduct their analyses successfully, it affected the formed chip and the machined surface. Moreover, they declared the hardship of selecting the optimum values of the ALE

parameters which can only be obtained by trials. This approach of using ALE with plasticity and damage models was adopted in this study. However, instead of tuning the ALE parameters, parameters of damage evolution laws, which are easier to be determined, were optimized to control the formed chip.

Yue et al. [3] successfully overcame excessive deformation that may lead to crash the analyses, in 3D cutting simulation of hard turning by adopting shear failure criteria and element deletion technique. They were able to predict cutting forces and residual stresses in good agreement with the experimental work.

Material properties used in J-C plasticity model may change for the same material from experimental work to another. For example, [9] compared the results obtained using two different sets of material properties, available in literature, of Ti-6Al-4V. They found that, the use of one set successfully predicted acceptable chip thickness while the other successfully predicted cutting forces. The same approach of checking the effects of material properties is also given in [10] where five different sets of materials constants were given for AISI 1045 steel.

In this paper, the effects of damage models and damage evolution parameters on the chip formation are studied. Two damage models, namely the Johnson-Cook (J-C) damage model and the dynamic shear failure model, are presented. These two models are used in metal cutting simulations. For the J-C damage model, it is necessary to apply a damage evolution law while the application of the shear failure model does not require a damage evolution law. One objective of this paper is to study the effects of the parameters of the damage evolution law, used with the J-C damage model, on chip formation. The paper also compares the chip formation obtained using the J-C damage model to that obtained using the shear failure model. Both of the models were applied to the metal cutting simulations of an Aluminum alloy, AL 1100. A finite element (FE) commercial package, ABAQUS, was used to conduct the simulations. Moreover, the effects of mesh size on the formed chip were studied, as well.

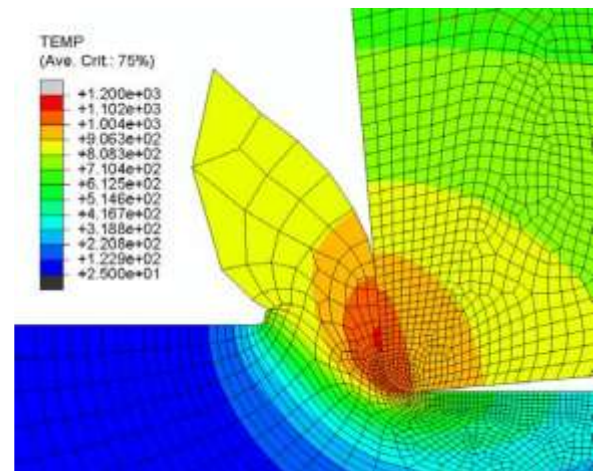


Figure 1: Material of the workpiece flows around the tool edge; no chip separation criterion is used [5].

II. MODEL DEFINITION

Figure 2 shows the 2D FE mesh of the workpiece and the cutting tool. The work piece is a rectangle of 5 mm length and 4 mm height. Plane strain quadrilateral four node reduced integration elements, CPE4R as designated in ABAQUS, were used. Fine mesh, of size $50 \mu\text{m} \times 50 \mu\text{m}$, were used in the region around the nose of the cutting tool while coarse mesh were used elsewhere. The mesh size in the fine mesh zone is comparable to the grain size of the workpiece material; grain sizes for Al alloys range from $10 \mu\text{m}$ to $1200 \mu\text{m}$ depending on the alloying element. The cutting tool was modelled as a rigid body, i.e. non-deformable.

Lagrangian boundary conditions, the default in ABAQUS, were applied to both the work piece and the cutting tool. The work piece was fixed in all direction at the lower and the left hand side. The cutting tool was fixed in Y-direction while it was allowed to move in negative X-direction with a constant speed of 30 m/min which is the value of the cutting speed.

Surface to surface contact algorithm by using penalty mechanical constraint is employed to the model. For the first surface, the tool surface is chosen and for the second surface, the workpiece surface with internal nodes, by defining a set of nodes in which the tool would engage during simulation, is chosen.

In order to control the excessive distortion experienced in metal cutting simulation, Arbitrary Lagrangian Eulerian (ALE) adaptive meshing facility, available in ABAQUS, was used. ALE combines the features of pure Lagrangian analysis in which the mesh follows the material, and Eulerian analysis in which the mesh is fixed spatially and material flows through the mesh.

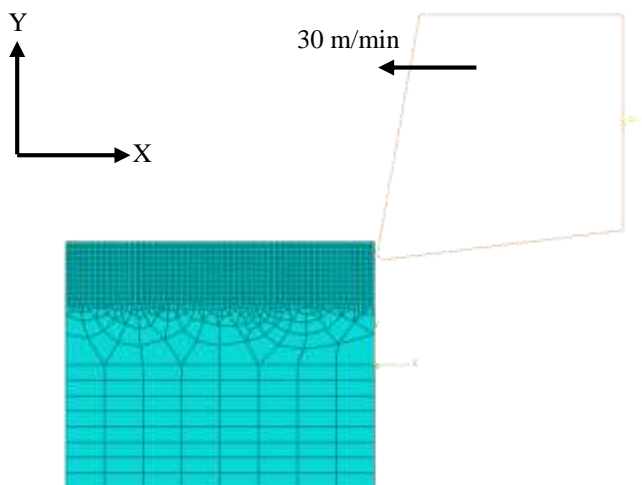


Figure 2: Finite Element model of the workpiece and the cutting tool.

TABLE 1: CUTTING SIMULATION CONDITIONS AND SPECIFICATIONS

Cutting speed	30 m/min
Cutting depth	0.3 mm
Tool rake angle	10°
Tool clearance angle	7°
Tool edge radius	0.1 mm

III. MATERIAL CONSTITUTIVE MODELS

The material used in this study is an Aluminum alloy (Al 1100). For high strain and/or high strain rate FE analyses, it is recommended to use Johnson-Cook plasticity model [2]. The J-C plasticity model describes the flow stress of a material with the product of strain, strain rate and temperature effects that are individually determined as given by Eq. (1). The temperature term was not used in this study. J-C plasticity model is given by

$$\sigma = (A + B(\varepsilon_{pl})^n) \left[1 + C \ln \left(\frac{\dot{\varepsilon}_{pl}}{\dot{\varepsilon}_{ref}} \right) \right] \left[1 - \left(\frac{T - T_{tr}}{T_{melt} - T_{tr}} \right)^m \right] \quad (1)$$

where A, B, n, C and m are material constants that can be determined experimentally at or below transition temperature. Values of these constants for Al 1100 are obtained from [4] and are given in Table 2. σ is the flow stress, ε_{pl} is the equivalent plastic strain at which σ is calculated, $\dot{\varepsilon}_{pl}$ is the plastic strain rate, $\dot{\varepsilon}_{ref}$ is the reference plastic strain rate, which is generally normalized to a strain rate of 1s^{-1} .

T is the current analysis temperature, T_{tr} is the transient temperature which is defined as the temperature at, or below which, there is no temperature dependence on the expression of the flow stress. T_{melt} is the melting temperature of the material.

TABLE 2: ALUMINUM ALLOY (AL 1100) MATERIAL CONSTANTS FOR THE CONSTITUTIVE EQUATIONS. [4].

Model	Material constants				
	A (MPa)	B (MPa)	n	C	m
J-C plasticity model	148	361	0.183	0.001	0.859
J-C damage model	d1	d2	d3	d4	d5
	0.071	1.248	-1.142	0.147	0.0

IV. DAMAGE MODELS

Chip separation can be modelled in ABAQUS by using progressive damage models or by using dynamic failure models. In the progressive damage models, after damage initiation, the material stiffness is degraded progressively according to the specified damage evolution response. The progressive damage models allow for a smooth degradation of the material stiffness, which makes them suitable for both quasi-static and dynamic situations [1]. Dynamic failure models are suitable for high-strain-rate dynamic problems. In dynamic failure model, once the damage initiation criterion has been met, the element is completely failed and removed from the model. A comparison is made, in this study, between the Johnson-Cook progressive damage model, referred to as J-C damage model in this article, and the dynamic shear failure model, referred to as shear failure model in this article.

A. J-C Damage Model

The J-C damage model is used for modeling material damage and failure in both quasi-static and dynamics in ABAQUS/Explicit. In this model the equivalent plastic strain at the onset of damage, ε_D^{pl} , is assumed to be of the form:-

$$\varepsilon_D^{pl} = \left[d_1 + d_2 \exp\left(d_3 \frac{p}{q}\right) \left[1 + d_4 \ln\left(\frac{\dot{\varepsilon}_{pl}}{\dot{\varepsilon}_{ref}}\right) \right] \left[1 - d_5 \left(\frac{T - T_{tr}}{T_{melt} - T_{tr}}\right)^m \right] \right] \quad (2)$$

where ε_D^{pl} is the equivalent plastic strain at the onset of damage, d_1 to d_5 are failure parameters, p is the mean stress, q is the von Mises stress, $\dot{\varepsilon}_{ref}$ is the reference strain rate, $\dot{\varepsilon}_{pl}$ is plastic strain rate, T is the current analysis temperature, T_{tr} is the transient temperature, T_{melt} is the melt temperature and m is a material constant. The effects of temperature is ignored in this study by setting $d_5=0.0$.

The criterion for damage initiation is met when ω_D equals to 1.0, where ω_D is a state variable that increases monotonically with plastic deformation. At each increment during the analysis the incremental increase in ω_D is computed as [1]:-

$$\Delta\omega_D = \frac{\Delta\varepsilon^{pl}}{\varepsilon_D^{pl}(-\dot{p}/q, \dot{\varepsilon}^{pl})} \geq 0.0 \quad (3)$$

When $\omega_D=1.0$, damage initiated and the damage parameter D , as defined in Eq. 4, is set to zero. The value of D is then increasing with the increase of plastic strain. An element is failed when D at an integration point reaches the value of 1.0. When $D=1.0$, the element is assumed to lose its load carrying capacity and behaves as liquid with zero stiffness. The damage evolution parameter D is calculated as:-

$$D = \sum \frac{\Delta\varepsilon^{pl}}{\varepsilon_D^{pl}} \quad (4)$$

where $\Delta\varepsilon^{pl}$ is the plastic strain increment calculated at the end of each integration step and ε_D^{pl} is plastic strain at the onset of damage calculated using Eq. (2).

Damage parameter calculated using Eq. (4) is mesh dependent as strain depends on the element size. To overcome this, a damage evolution law based on equivalent displacement is presented. The relationship between damage and displacement can be linear, exponential or presented in a tabular form. The linear form is:

$$\dot{D} = \frac{L\dot{\varepsilon}^{pl}}{\bar{u}_f^{pl}} = \frac{\dot{\bar{u}}^{pl}}{\bar{u}_f^{pl}} \quad (5)$$

where, \dot{D} is the damage rate, L is a characteristic length of the element used, $\dot{\varepsilon}^{pl}$ is the rate of the equivalent plastic strain, \bar{u}_f^{pl} is the equivalent plastic displacement at failure provided by the user, $\dot{\bar{u}}^{pl}$ is the rate of equivalent plastic displacement. For plane strain elements, the characteristic length is a typical length of a line across the element [1].

Once the equivalent plastic displacement, \bar{u}^{pl} , reaches the value of the equivalent plastic displacement at failure, \bar{u}_f^{pl} , the damage parameter D reaches 1.0 and the material stiffness is fully degraded and the element is removed.

B. Shear Failure Model

For quasi-static and dynamic analyses, ABAQUS offered failure models such as ductile criterion, Johnson-Cook criterion and other criteria for sheet metal analyses. However, for high-strain-rate dynamic problems, two additional models are offered: the *shear failure model*, which is driven by plastic yielding, and the *tensile failure model*, which is driven by tensile loading [1].

The dynamic shear failure model is based on the value of the equivalent plastic strain at element integration points. Failure is assumed to occur when the damage parameter, ω , exceeds 1.0. For the shear failure model, the damage parameter, ω , is defined as:

$$\omega = \frac{\varepsilon_0^{pl} + \sum \varepsilon^{pl}}{\varepsilon_D^{pl}} \quad (6)$$

where ε_0^{pl} is any initial value of the equivalent plastic strain, ε^{pl} is an increment of the equivalent plastic strain, ε_D^{pl} is the strain at failure (given in Eq. 2), and the summation is performed over all increments of the analysis[1].

The strain at failure, ε_D^{pl} , is given in Eq. 2. Again, if Eq. 2 is used to determine ε_D^{pl} , material constants d_1 to d_5 must be provided.

V. FINITE ELEMENT ANALYSES

Chip separation was modelled using J-C damage model at different values of \bar{u}_f^{pl} . Moreover, it was modelled using shear failure model. The cutting parameters, such as feed, speed, etc. were kept the same in all of the analyses. Firstly, the effects of the damage evolution parameter \bar{u}_f^{pl} on the chip formation was studied. Secondly, mesh study was carried out at the value of $\bar{u}_f^{pl}=0.01$ mm by using different mesh sizes in the fine mesh region of the model. Results obtained from the J-C model was then compared to those obtained from the shear failure model.

A. J-C Damage Model

1) Effects of \bar{u}_f^{pl} as the damage evolution parameter.

Using J-C damage model, once the damage initiated at an integration point of an element, a *damage evolution* law is applied. Damage evolution laws available in ABAQUS are the equivalent plastic displacement and fracture dissipations energy. In this study, the equivalent plastic displacement is used as the damage evolution law.

The mesh size in the fine mesh zone of the work piece is 0.05 mm. Therefore, a value of the equivalent displacements at failure, \bar{u}_f^{pl} , close to that size, was initially, selected. It is

worth noting that setting the value of \bar{u}_f^{pl} equal to zero is not recommended as it causes a sudden drop of the stress at the material point that can lead to dynamic instabilities [1]

Figure 3 shows the chip formed at $\bar{u}_f^{pl}=0.01, 0.05, 0.1$ and 0.5 mm. It can be seen that, the chip thickness increases as the value of \bar{u}_f^{pl} increases. Moreover, more mesh distortion can be seen at high values of \bar{u}_f^{pl} . Although the ALE was used, to control mesh distortion, the analyses at \bar{u}_f^{pl} of 0.1 and 0.5 mm

were crashed prematurely due to excessive mesh distortion. It can also be seen that the size of the plastically deformed material at the start of the cutting process, the circled region in the figure, increases as the \bar{u}_f^{pl} increases. These results highlight the importance of the value of \bar{u}_f^{pl} . Therefore, it is recommended to correlate the FE results with experimental results in order to determine an optimum value of \bar{u}_f^{pl} .

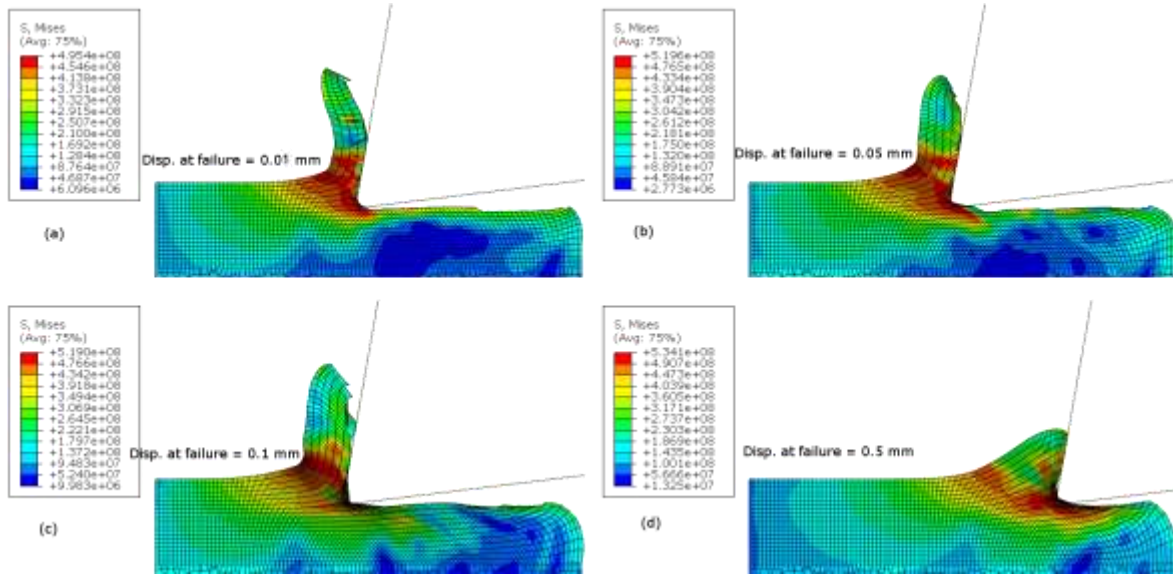


Figure 3: Results obtained using the J-C ductile damage model with different values of the equivalent displacement at failure as the damage evolution parameter.

2) Effects of Mesh Size

One of the purposes of using the equivalent displacement at failure as a damage evolution law is to minimize the mesh dependency of the results [1]. To investigate this, FE analyses with different mesh sizes were carried out. The results of these analyses are shown in Figure 4 for mesh sizes, at the fine mesh zone, of $0.05, 0.08, 0.1$ and 0.3 mm, respectively. It can be seen that, in terms of stress, the results are practically mesh independent for mesh size less than 0.1 mm. However, it is

noticeable that the chip is continuous for the finest mesh, 0.05 mm, while it is fragmented at other sizes. Remembering that, the thickness of the chip is affected by the equivalent displacement at failure selected, as well. Results obtained for the very coarse mesh, Figure 4 (d), are not comparable to that for the fine mesh. Again, the plastically deformed zone at the beginning of the cutting process increases as the mesh size increases.

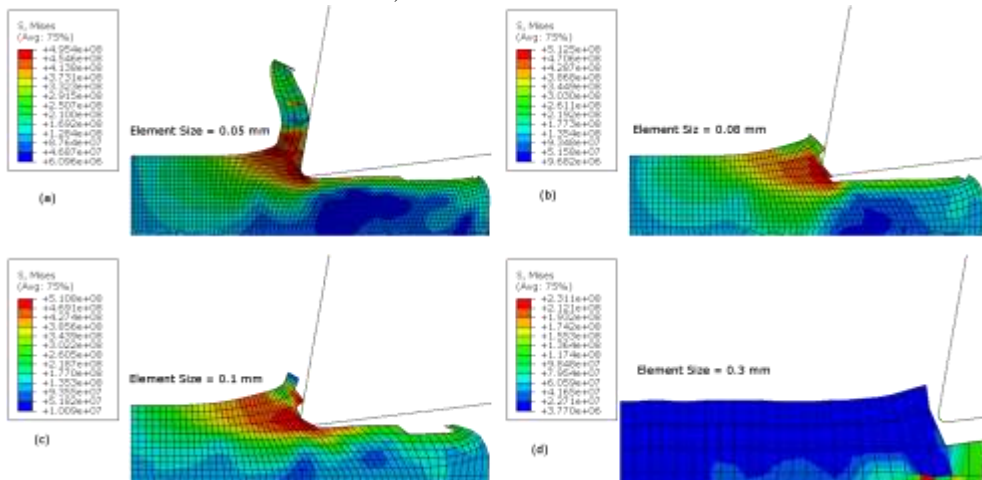


Figure 4: Effects of mesh size on the chip formation and its continuity.

B. Dynamic Shear Failure Model

When using the dynamic shear failure model as a damage (and failure) model, no damage evolution is needed. Moreover, the material constants used in J-C damage model, d_1 to d_5 are needed. The results obtained using the shear failure model is compared to those obtained using J-C damage model with damage evolution, see Figure 5. The FE model used in both cases is the same and all of the simulation conditions, i.e. material properties, cutting speed, were kept the same. The differences are that, the shear failure model was presented by editing the .inp file; it is not supported in ABAQUS\CAE. From Figure 5, it can be seen that both models produce almost same chip morphology. However, chip thickness ratio, the

deformed chip thickness divided by the undeformed chip thickness, is higher in shear model rather than the J-C model. Figure 6 compares the normalised cutting and feed forces for the two models; the J-C damage model and the shear failure model. The forces are normalised with respect to the greatest value of each of them. It can be seen that the cutting forces obtained from both models are quite similar with little variation in the case of shear failure model. In addition, although the fluctuations in the feed force for the two models are significant, general trends obtained from the two models are quite similar results.

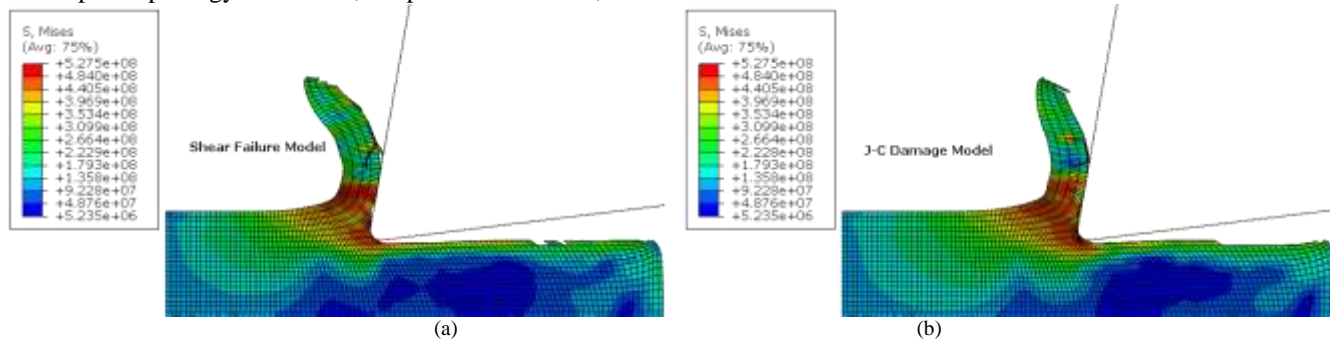


Figure 5: Chip formed using (a) shear failure model and (b) J-C damage model.

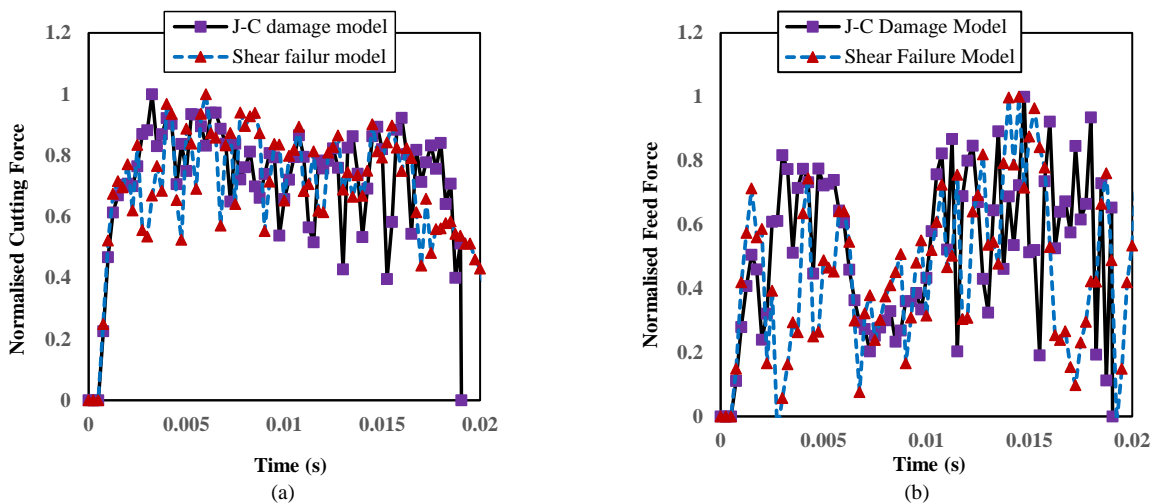


Figure 6: Normalised (a) cutting forces and (b) feed forces for the J-C damage model and the shear failure model.

VI. CONCLUSIONS

ABAQUS FE package was used successfully to simulate the cutting process of Al 1100. The analyses involved chip formation, therefore, two models with element deletion were used: (i) J-C ductile damage model and (ii) shear failure model. When J-C damage model was applied, damage evolution law must be used. The damage evolution parameter used was the equivalent displacement at failure, \bar{u}_f^{pl} . The initial value of \bar{u}_f^{pl} is about one-fifth of the mesh size in the fine region. It was found that, the FE results are very sensitive to the value of \bar{u}_f^{pl} and to the mesh size at the chip zone of the workpiece model. Therefore, it is recommended to tune up

both the initial value of the \bar{u}_f^{pl} and mesh size, at the chip zone, until the FE formed chip has almost the same morphology as the experimentally obtained chip.

It can be concluded that, the formed chip is sensitive to the mesh size. The Chip is continuous when fine meshes were used while it is fragmented when coarse meshes were used.

The results obtained using the J-C damage model and those obtained using the shear failure model is in very good agreement. Therefore, in order to avoid the sensitivity of the damage evolution parameter, it is recommended to apply the shear model to run the FE cutting simulations.

To sum up, it is very important to consider the effects of the values of \bar{u}_f^{pl} and the correlation between this values and

the mesh size of the model. Alternatively, shear failure model can be used to avoid the application of \bar{u}_f^{pl} .

VII. REFERENCES

- [1] ABAQUS, ABAQUS/CAE Version 6.14 documentation, 2014.
- [2] G. R. Johnson, and W.H. Cook, "A constitutive model and data for metals subjected to large strains, high strain rates and high temperatures," in The 7th International Symposium on Ballistics, The Hague, The Netherlands, 1983.
- [3] C. X. Yue, X. L. Liu, D. K. Jia, S. Y. Ji, and Y. S. Zhai, "3D Finite Element Simulation of Hard Turning," *Advanced Materials Research*, 2009, 69-70.
- [4] M. Fathipour, P. Zoghipour, J. Tarighi, and R. Yousefi, "Investigation of Reinforced Sic Particles Percentage on Machining Force of Metal Matrix Composite," *Modern Applied Science*, 2012, 6(8).
- [5] Özel, and E. Zeren, "Finite Element Method Simulation of Machining of AISI 1045 Steel With A Round Edge Cutting Tool," in The 8th CIRP International Workshop on Modeling of Machining Operations, Chemnitz, Germany, May 2005.
- [6] T. T. Öpöz and X. Chen, "Finite element simulation of chip formation," in CEARC'10, University of Huddersfield, Huddersfield, 2010.
- [7] E. G. Ng and D. K. Aspinwall, "Modelling of hard part machining," *Journal of Materials Processing Technology*, 2002, 127(2).
- [8] D. C. Bowes, "Numerical Modelling of Ti6Al4V Machining: A Combined FEA and Unified Mechanics of Cutting Approach, in Department of Mechanical Engineering," University of Stellenbosch, Stellenbosch University: Stellenbosch University, 2013.
- [9] Y. Zhang, J. C. Outeiro, and T. Mabrouki, "On the Selection of Johnson-cook Constitutive Model Parameters for Ti-6Al-4 V Using Three Types of Numerical Models of Orthogonal Cutting," *Procedia CIRP*, 2015, 31
- [10] J. Zouhar, and M. Piska, "Modelling the orthogonal machining process using cutting tools with different geometry," *Modern Machinery Science Journal*, 2008.